Geophysical Research Letters

Supporting Information for

Exceptional 20th century ocean circulation in the Northeast Atlantic

Peter T. Spooner[1]*, David J. R. Thornalley[1,2]*, Delia W. Oppo[2], Alan D. Fox[3], Svetlana Radionovskaya[1], Neil L. Rose[1], Robbie Mallett[1], Emma Cooper[1], J. Murray Roberts[4]

[1]Department of Geography, University College London, Pearson Building, Gower Street, London, WC1E 6BT, UK

[2]Department of Geology and Geophysics, Woods Hole Oceanographic Institution, Woods Hole, MA 02543-1050, USA

[3]SAMS, Scottish Marine Institute, Oban, Argyll, PA37 1QA, UK

[4]School of Geosciences, University of Edinburgh, The King's Buildings, James Hutton Road, Edinburgh, EH9 3FE, UK

Contents of this file

Additional Supporting Information (Files uploaded separately)

Introduction

This supporting information file contains supplementary detail on the methods and sediment cores used in this study. Supporting data are available as excel files. These data are also available from the World Data Service for Paleoclimatology (https://www.ncdc.noaa.gov/paleo/study/29030). Particle tracking data are available from Zenodo (https://zenodo.org/record/3727170).

Text S1:

Supplementary Methods

1. Sediment cores

Multi cores were selected based on previously existing age control data and the relative presence/absence of sediment disturbance. For all multi cores analysed in this study, we utilized the 'A' and/or 'B' cores from each sample site (Table S1). We consider the core EN539-MC16-A to offer the most robust sediment archive, because it was sampled immediately upon collection with the core top relatively undisturbed, and does not show strong evidence for bioturbation or significant volcanic sediment input from Iceland.

2. Age models

For each 'B' multicore, ^{210}Pb activity was measured in the bulk sediment at a resolution of every 1-3 cm for the upper 20-30 cm at the Woods Hole Oceanographic Institution Coastal Systems Group facility. Radiocarbon ages were based on several hundred specimens of planktonic foraminifera (mixed or *G. bulloides* only, as specified in the supplementary tables) found in the 'A' cores (and RAPID-17-5P). Radiocarbon dates were measured at the National Ocean Sciences Accelerator Mass Spectrometry (NOSAMS) and the Keck-Carbon Cycle AMS facility, University of California, Irvine. Radiocarbon ages were calibrated

using the MARINE13 curve (Reimer et al., 2013), individually using Calib7.1 (Stuiver et al., 2020), and by using a Bayesian framework in OxCal with a Poisson deposition model (Ramsey, 2008). In all cases we used a standard reservoir age of 400 years (ΔR = 0). The comparison between the A and B cores was confirmed by repeat analysis of select species data in each (e.g. Figs. S1, S2). Similarly, species counts were used to confirm that the base of EN539-MC16-A and the top of RAPID-17-5P do not likely overlap in age. The age model for RAPID-17-5P therefore constrains the basal age of EN539-MC16-A (Fig. S7).

Given the difficulty of calibrating radiocarbon ages in the last 200 years, our favoured age models spanning that time interval are based on the simplest assumption of constant dry mass accumulation rate derived from a linear fit through the ^{210}Pb dates (Fig. S7) with the age of the sediment water interface set to the date of collection (Table S1). The ^{14}C dates that fall within this problematic time window are all consistent with these age models if the modern surface ocean ^{14}C reservoir age of 400 years is allowed to vary by ± 85 years (Fig. S7), within the range of regional variability (Eiríksson et al., 2004). For deeper samples, we maintain the assumption of constant dry mass accumulation when interpolating between pairs of ^{14}C dates. We note that because the ^{210}Pb dates are from the 'B' cores, our preferred age model for the 'A' cores (Fig. S7) may not pass through these dates due to differences in percent water content of the different core materials. Age models for the 'B' cores (Data S1) are consistent with these ^{210}Pb measurements.

3. Faunal assemblages

Multi-cores were sliced at 0.5 cm intervals, weighed wet, freeze dried and weighed again, and then wet sieved through a 63 μm mesh in distilled water. Coarse fraction samples were then dried at 40 ^{o}C. Dry coarse fraction was then

sieved to separate the >150 μm size fraction. RAPID-17-5P samples are 0.5 or 1 cm wide. Planktonic foraminifera were identified to species level following the taxonomy of Brummer & Kucera, (2015) and counted in this dried fraction, in splits of $1/2^n$ of the total sample, where n is the number required to obtain a split containing ~300 total foraminifera. In EN539-MC16-A and EN539-MC14-A, the full species assemblage was analysed. In remaining cores, the key species *Turborotalita quinqueloba* and *Orbulina universa* were counted.

Simply counting the rare subtropical species O. universa in the >150 μm size fraction splits of ~300 foraminifera did not result in any specimens for many samples. Therefore, we searched the >250 μm size fraction of the whole (not split) samples for this species, which resulted in a greater number of individuals and therefore more robust count statistics. We report these data as percentages by assuming that the number of individuals in the 150-250 μm is negligible. Our reported percentage value is therefore a lower estimate.

For the SIMMAX temperature reconstruction, temperatures for analogues (annual mean, 1955-2012) were obtained from the World Ocean Atlas (Locarnini et al., 2014). Analogues were restricted to the North Atlantic and were taken from the 'ForCenS' compilation (Siccha & Kucera, 2017). Ten analogues were used to determine temperature (Spielhagen et al., 2011), weighted by distance from the same site. Method uncertainty is ±1 °C (Pflaumann et al., 1996). We elected not to use a temporal calibration, because beyond the observational period the assemblage rapidly diverges to one outside the possible calibration range. However, we note that the recent decadal temporal changes inferred by our approach are a close match to reanalysis data from the region, albeit lower in magnitude (Fig. 2).

4. $\delta^{15}N$ measurements

After gentle crushing and mixing, around 100 mg of sediment were taken from dried samples. These aliquots were then subjected to two treatments in 1M HCl in order to remove carbonates, followed by de-ionized water rinses. Approximately 16 mg of each treated and dried sample was weighed into tin capsules in preparation for measurement.

The $\delta^{15}N$ of each sample was measured at the University of Cambridge. Samples are analysed for using a Costech Elemental Analyser attached to a Thermo DELTA V mass spectrometer in continuous flow mode.

Samples were flash combusted in the combustion reactor at 1500 ^{o}C. The combustion products are carried by a constant flow of Helium "carrier gas" through an oxidation catalyst of Chromium trioxide and then silver coated cobaltic oxide both kept at 1020 ^{o}C. The excess of oxygen not used for the combustion is removed in the "reduction tube" of metallic copper at a temperature of 650 ^{o}C, and at this temperature the nitrogen oxides coming from the combustion process are reduced to elemental nitrogen. Water is removed by passing the gases through a tube containing magnesium perchlorate. The gases then flow through the gas chromatographic (GC) separation column at constant temperature of 45 +/- 0.1 ^{o}C and into the mass spectrometer for analysis. Reference standards from IAEA in Vienna are run at intervals throughout the sequence and these values are used to calibrate to the international standards for $^{14}N/^{15}N$. Precision of analyses is better than ± 0.1 ‰ for $^{14}N/^{15}N$.

5. Particle tracking experiments

VIKING20 is a 1/20th degree ocean model, forced by a historical simulation of the atmosphere: CORE2 (Griffies et al., 2009). The reverse tracks of 113200 particles were simulated with the ARIANE software (Döös, 1995) modified to include independent vertical motion of particles. Particles were seeded at the seabed in

10 km x 10 km boxes centered on MC16-A/17-5P and RAPID-21-3K. They rose at 100 m/day (Takahashi & Be, 1984) and were then allowed to drift freely within the upper 100 m of the water column for one month (i.e. a reasonable lifespan for many species of planktic foraminifera). In secondary experiments, we modelled particles that rose from the seabed at both 100 m/day and 1000 m/day, and were confined to either the upper 30 m or 100 m. We ran each different combination of these parameters. None of these experiments made a substantial difference to the final results.

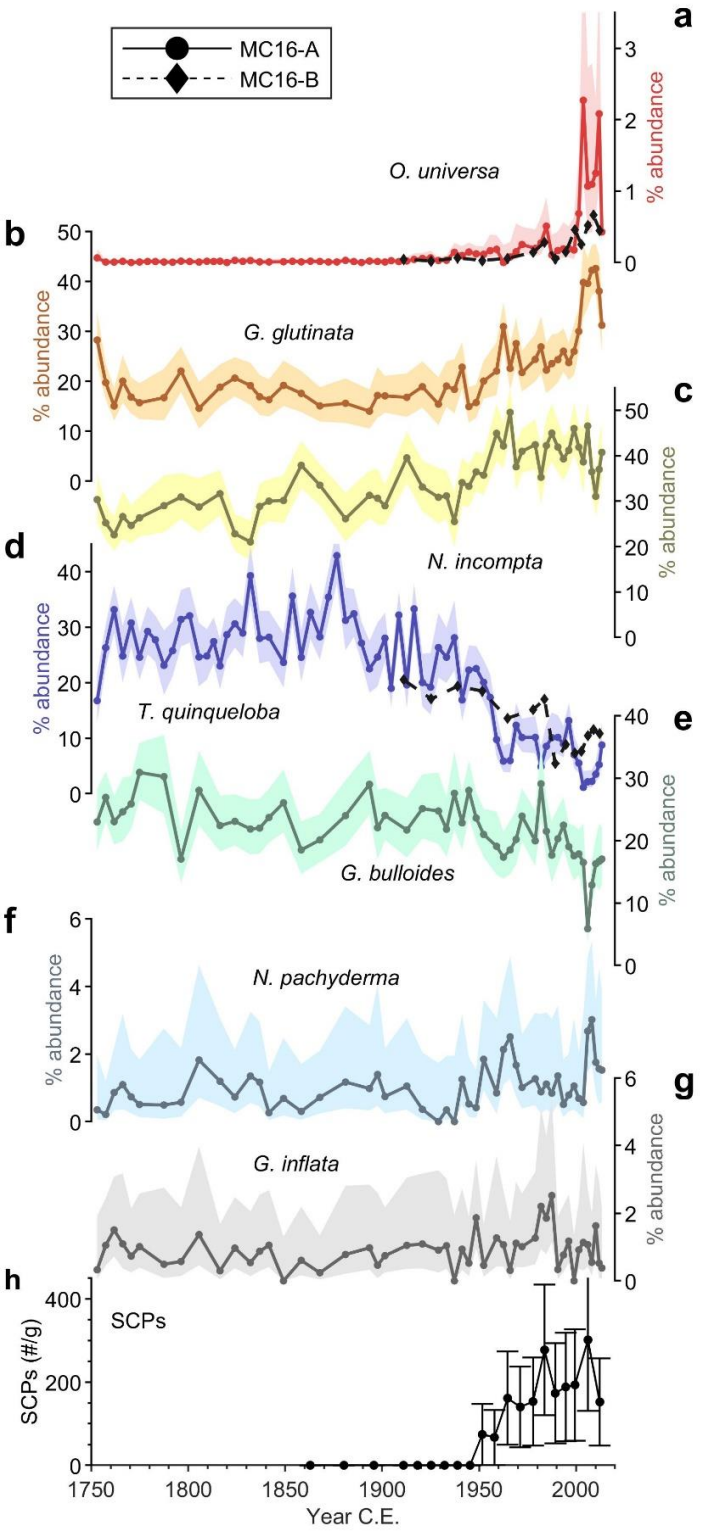

Figure S1: Faunal assemblage data for the core EN539-MC16-A, showing the relative % abundances of a) *Orbulina universa*, b) *Globigerinita glutinata*, c) *Neogloboquadrina incompta* d) *Turborotalita quinqueloba*, e) *Globigerina bulloides*, f) *Neogloboquadrina pachyderma*, g) *Globorotalia inflata*, in the >150 µm size fraction (percent *O. universa* is calculated as the total number of specimens in the >250 µm size fraction divided by the number of foraminifera >150 µm). h) concentration of spheroidal carbonaceous particles (used to assess the age model, see methods) for reference. Shading on faunal abundance data indicates 2σ confidence intervals.

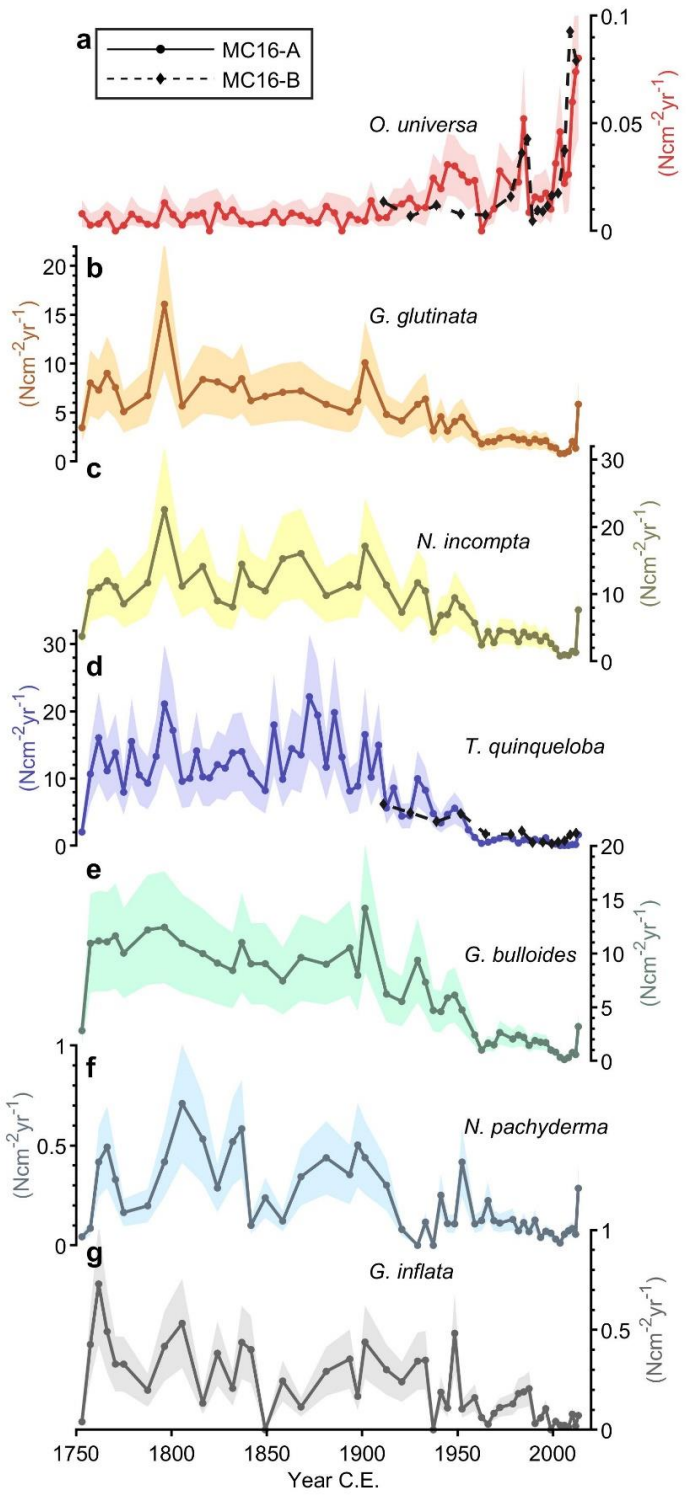

Figure S2: Faunal assemblage data for the core EN539-MC16-A, showing the fluxes of a) *Orbulina universa*, b) *Globigerinita glutinata*, c) *Neogloboquadrina incompta* d) *Turborotalita quinqueloba*, e) *Globigerina bulloides*, f) *Neogloboquadrina pachyderma*, g) *Globorotalia inflata*, in the >150 µm size fraction (percent *O. universa* is calculated as the total number of specimens in the >250 µm size fraction divided by the number of foraminifera >150 µm. Shading on faunal abundance data indicates 2σ confidence intervals.

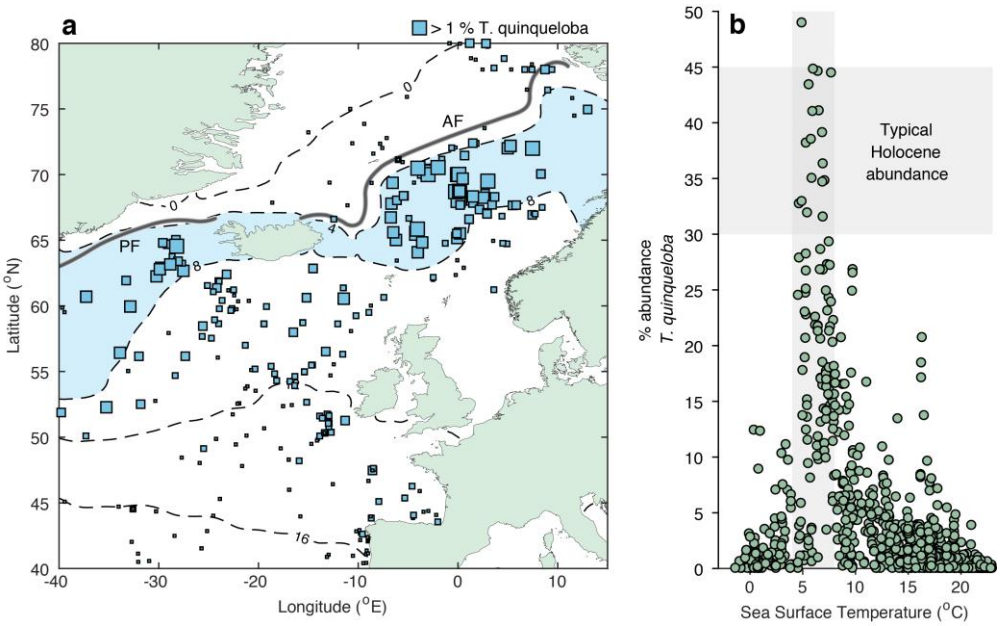

Figure S3: Relative abundances of *T. quinqueloba* in the >150 µm fraction of core top sediments from the Northeast Atlantic. a) Core top locations. Symbols are shown for every site with *T. quinqueloba* >1 %, with width proportional to relative abundance. Modern SSTs (annual mean, 1955-2012, 10m depth) from the World Ocean Atlas (Locarnini et al., 2014) are plotted as contours. The approximate and relevant positions of the Arctic (AF) and Polar Fronts (PF) are shown by the thick grey lines (Blindheim & Østerhus, 2005; Kostianoy & Nihoul, 2009; Piechura & Walczowski, 1995; Swift & Aagaard, 1981). b) The relationship between SST and *T. quinqueloba* relative abundance in the Northeast Atlantic. High abundances typical of the values in pre-1800 16MC/5P are found where SSTs are 4-8 °C. SST during the warm early 2000s was ~8.5-10 °C. Note that for the core top samples, high abundances of *T. quinqueloba* are exclusively found in low temperature environments, whereas low abundances are found throughout the temperature range. Therefore, the high abundances in 16MC/5P suggest low temperatures for the northern Iceland Basin, despite the other cores having lower *T. quinqueloba* abundances.

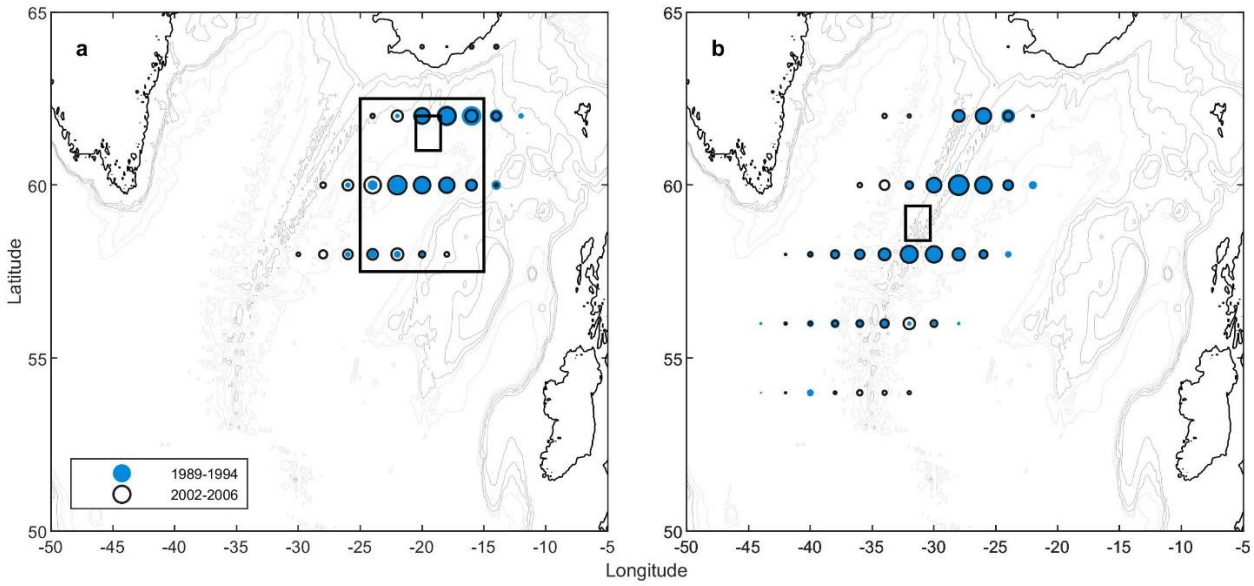

Figure S4: Results of particle tracking experiments showing the locations of particles one month before deposition on the seabed for a) MC16/17-5P and b) RAPID-21-3K. Size of symbols is proportional to the number of particles found in each 2°x2° box. Results are shown for the periods 1989-1994 (blue) and 2002-2006 (pink), periods of different SPG activity. The large black box shows the area used to calculate the mean annual climatological SST experienced by the particles. The small black box is the area covered by the particles on the seabed at the start of each experiment.

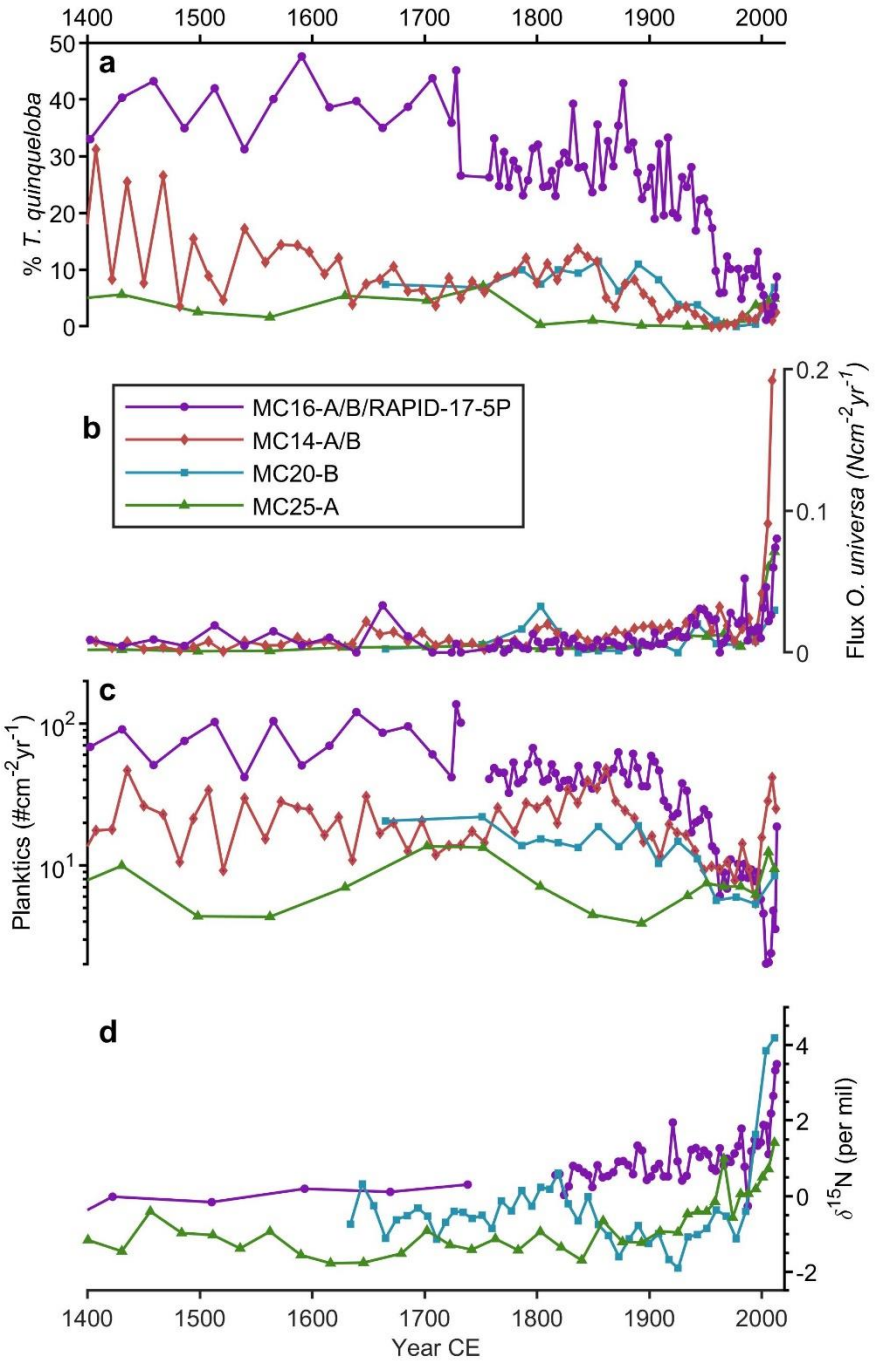

Figure S5: Comparison of key data from four sediment core locations in the northern Iceland Basin (for core locations see Fig. 1). Counting methods and size fractions were the same for all cores. a) Relative % abundance of *T. quinqueloba*; b) Flux (number per cm^2 per year) of *O. universa*; c) The flux (number per cm^2 per year) of planktonic foraminifera to the sediment; d) Nitrogen isotope ratios in bulk sediment.

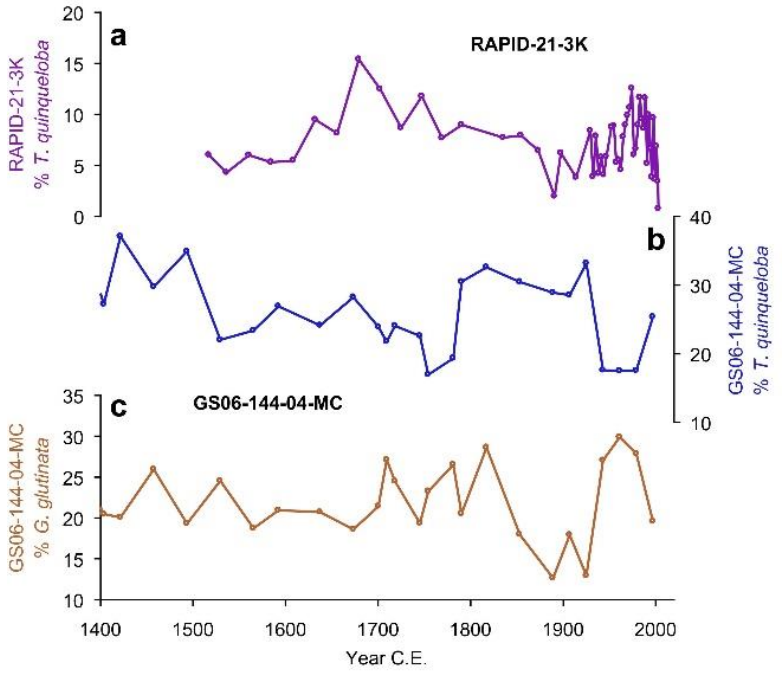

Figure S6: Comparison of selected faunal data from Reykjanes Ridge core sites, located within the SPG to the southwest of the Iceland Basin cores. a) *T. quinqueloba* abundance from RAPID-21-3K. Faunal data were collected as part of this study. The age model is based on published radiocarbon ages and ^{210}Pb dating (Miettinen et al., 2011). While the modern abundance drops close to zero percent (i.e. similar to Iceland Basin cores), such a change does not appear to be exceptional for this core. b) *T. quinqueloba* % abundance and c) *G. glutinata* % abundance from GS06-144-04-MC (Perner et al., 2017).

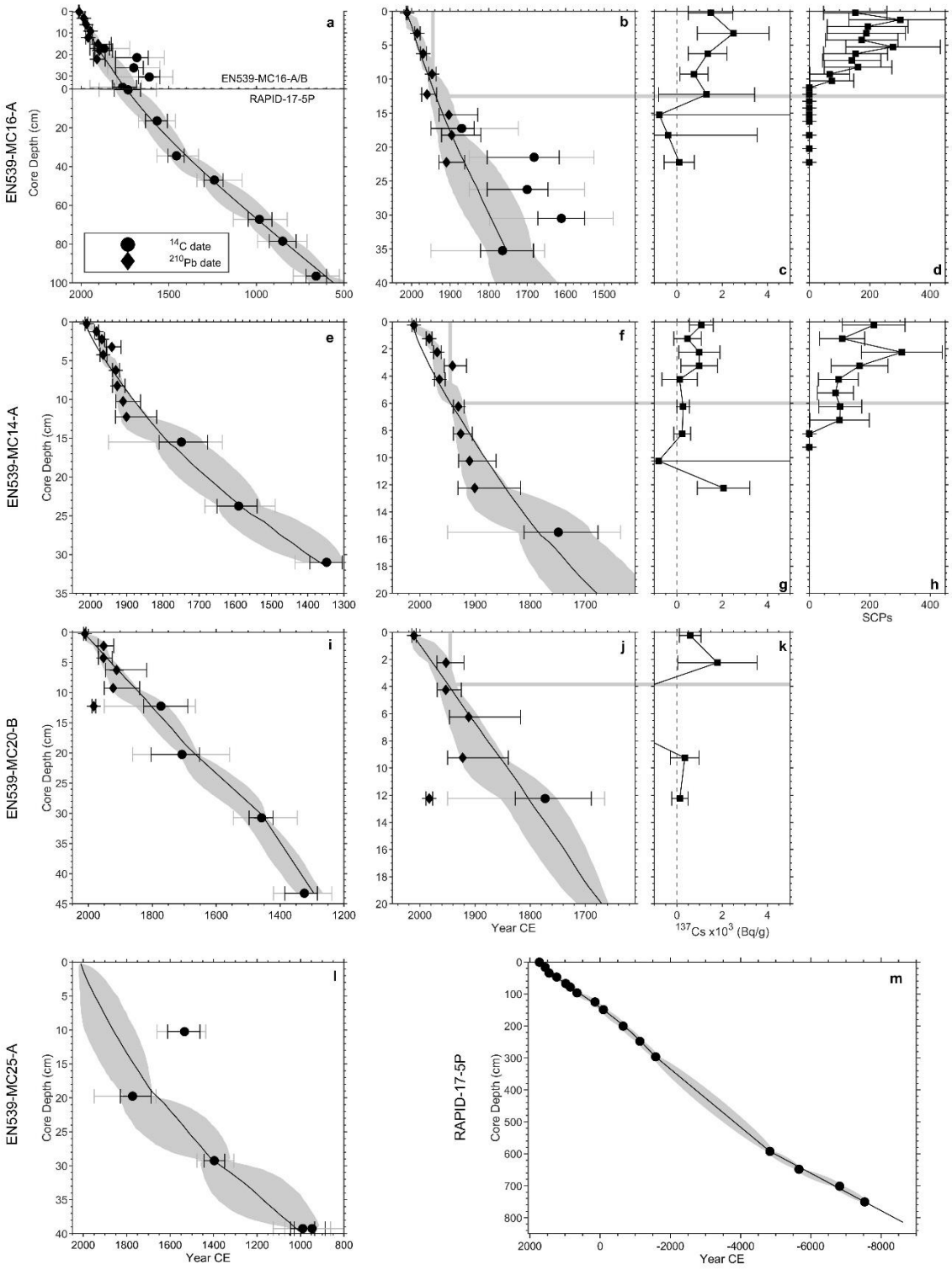
EN539-MC16-A
EN539-MC14-A
EN539-MC20-B
EN539-MC25-A
RAPID-17-5P
Core Depth (cm)
EN539-MC16-A/B
RAPID-17-5P
^{14}C date
^{210}Pb date
SCPs
Year CE
^{137}Cs x10^{3} (Bq/g)
a
b
c
d
e
f
g
h
i
j
k
l
m

Figure S7: Age models for the cores EN539-MC16-A (a-d), EN539-MC14-A (e-h), EN539-MC20-B (i-k), EN539-MC25-A (l) and RAPID-17-5P (m). ^{210}Pb (measured in MC16-B and MC14-B) and ^{14}C data (a,b,e,f,i,j,l,m) were used to construct the age models (see methods). The first presence of ^{137}Cs (c,g,k) and rapid increases in SCPs (d,h) after the 1950s are consistent with this approach. We prefer the oldest radiocarbon age in MC16-A to the three above it (b) because it fits well with the sedimentation rate estimated using the ^{210}Pb ages, and it is consistent with the topmost ages of RAPID-17-5P (a). RAPID-17-5P and MC16-A were taken from within 100m of one another, and their respective faunal assemblages suggest that they do not overlap in time. This provides an additional constraint on the oldest age for MC16-A. Discrepancy of ^{210}Pb ages near the core top of MC14-A may be related to a high abundance of volcaniclastic grains from 3-8 cm. Black and grey error bars represent the 1 sigma and 2 sigma age ranges respectively. Grey shading represents the age uncertainty obtained from OxCal. For RAPID-17-5P, error bars are smaller than the symbols. The age model for the section from 0-300 cm was fit to the radiocarbon data using a 6th order polynomial. Segments for the lower sections were linearly fit. Data can be found in the supplementary data files, which include published data (Moffa-Sanchez et al., 2014) for completeness.

Core	Collection date	Latitude (ºN)	Longitude (ºW)	Depth (m)	Core length (m)	Gear type*
EN539-MC16-A	28/05/2014	61.4831	19.5361	2311	0.35	MC
EN539-MC16-B	28/05/2014	61.4831	19.5361	2311	0.28	MC
EN539-MC14-A	28/05/2014	61.3465	20.3484	2274	0.31	MC
EN539-MC14-B	28/05/2014	61.3465	20.3484	2274	0.20	MC
EN539-MC20-B	29/05/2014	61.6715	21.7326	1711	0.22	MC
EN539-MC25-A	30/05/2014	62.6125	20.6358	1310	0.49	MC
RAPID-17-5P	09/07/2004	61.4817	19.5360	2303	14.39	P
RAPID-21-3K	12/07/2004	57.2715	27.5488	2630	0.65	K

Table S1: Details of core sites for which new data was gathered for this study. * Multi core (MC); Piston core (PC); Kasten core (K).

(Data Sets S1 – S16 included in a single Excel file dS1)

Data Set S1. EN539-MC16-A data faunal count data. Core collected on 28/05/2014 at 61.4831ºN, 19.5361ºW, 2311 m depth. Note that *O. universa* (%) was calculated as the total number of specimens >250 µm as a percentage of the total number of planktonic foraminifera >150 µm in the sample. Because this latter number is subject to splitting uncertainty, the sum of the percentages listed below may not be exactly 100 % in all cases.

Data Set S2

EN539-MC16-B data. Core collected with MC16-A.

Data Set S3

EN539-MC16-A radiocarbon dates.

Data Set S4

EN539-MC16-B ^{210}Pb data.

Data Set S5

RAPID-17-5P faunal count data. Core collected at 61.4817° N, 19.5360° W, 2303 m depth.

Data Set S6

RAPID-17-5P radiocarbon dates.

Data Set S7

EN539-MC14-A faunal count data. Core collected on 28/05/2014 at 61.3465°N, 20.3484°W, 2274 m depth.

Data Set S8

EN539-MC14-B. Core collected with MC14-A.

Data Set S9

EN539-MC14-A radiocarbon dates.

Data Set S10

EN539-MC14-B ^{210}Pb data.

Data Set S11

EN539-MC20-B faunal count data. Core collected on 29/05/2014 at 61.6715°N, 21.7326°W, 1711 m depth.

Data Set S12

EN539-MC20-B radiocarbon dates.

Data Set S13

EN539-MC20-B ^{210}Pb data.

Data Set S14

EN539-MC25-A faunal count data. Core collected on 30/05/2014 at 62.6125°N, 20.6358°W, 2274 m depth.

Data Set S15

EN539-MC25-A radiocarbon dates.

Data Set S16

RAPID-21-3K planktic foraminifera faunal count data.

References

Blindheim, J., & Østerhus, S. (2005). The Nordic Seas, Main Oceanographic Features. In The Nordic Seas: An Integrated Perspective: Oceanography, Climatology, Biogeochemistry, and Modeling (pp. 11–37). Wiley Blackwell. https://doi.org/10.1029/158GM03

Brummer, G. J. A., & Kucera, M. (2015). Taxonomy of extant planktonic foraminifera, SCOR/IGBP WG138; August 2015. In H. Spero & M. Kucera (Eds.), *SCOR/IGBP Working Group 138: Planktonic Foraminifera and Ocean Changes. Final Workshop & Short Course on Culturing Planktonic Foraminifera* (p. 8). California.

Döös, K. (1995). Interocean exchange of water masses. *Journal of Geophysical Research*, *100*(C7), 13499. https://doi.org/10.1029/95JC00337

Eiríksson, J., Larsen, G., Knudsen, K. L., Heinemeier, J., & Símonarson, L. A. (2004). Marine reservoir age variability and water mass distribution in the Iceland Sea. *Quaternary Science Reviews*, *23*(20-22 SPEC. ISS.), 2247–2268. https://doi.org/10.1016/j.quascirev.2004.08.002

Griffies, S. M., Biastoch, A., Böning, C., Bryan, F., Danabasoglu, G., Chassignet, E. P., et al. (2009). Coordinated Ocean-ice Reference Experiments (COREs). *Ocean Modelling*, *26*(1–2), 1–46. https://doi.org/10.1016/J.OCEMOD.2008.08.007

Kostianoy, A. G., & Nihoul, J. C. J. (2009). Frontal Zones in the Norwegian, Greenland, Barents and Bering Seas. In Influence of Climate Change on the Changing Arctic and Sub-Arctic Conditions (pp. 171–190). https://doi.org/10.1007/978-1-4020-9460-6_13

Locarnini, R. A., Mishonov, A. V., Antonov, J. I., Boyer, T. P., Garcia, H. E., Baranova, O. K., et al. (2014). World Ocean Atlas 2013, Volume 1: Temperature. In S. Levitus & A. Mishonov (Eds.), *NOAA Atlas NESDIS 73* (p. 40).

Miettinen, A., Koç, N., Hall, I. R., Godtliebsen, F., & Divine, D. (2011). North Atlantic sea surface temperatures and their relation to the North Atlantic Oscillation during the last 230 years. *Climate Dynamics*, *36*(3), 533–543. https://doi.org/10.1007/s00382-010-0791-5

Moffa-Sanchez, P., Born, A., Hall, I. R., Thornalley, D. J. R., & Barker, S. (2014). Solar forcing of North Atlantic surface temperature and salinity over the past millennium. *Nature Geoscience*, *7*(April), 275–278. https://doi.org/10.1038/NGEO2094

Perner, K., Moros, M., Jansen, E., Kuijpers, A., Troelstra, S. R., & Prins, M. A. (2017). Subarctic Front migration at the Reykjanes Ridge during the mid- to late Holocene: Evidence from planktic foraminifera. *Boreas*, *47*(1), 175–188. https://doi.org/10.1111/bor.12263

Pflaumann, U., Duprat, J., Pujol, C., & Labeyrie, L. D. (1996). SIMMAX: A modern analog technique to deduce Atlantic sea surface temperatures from planktonic foraminifera in deep-sea sediments. *Paleoceanography*, *11*(1), 15–35. https://doi.org/10.1029/95PA01743

Piechura, J., & Walczowski, W. (1995). The Arctic Front : structure and dynamics.

Oceanologia, 37(1), 47–73.

Ramsey, C. B. (2008). Deposition models for chronological records. *Quaternary Science Reviews*, *27*(1–2), 42–60. https://doi.org/10.1016/j.quascirev.2007.01.019

Reimer, P. J., Bard, E., Bayliss, A., Beck, J. W., Blackwell, P. G., Bronk Ramsey, C., et al. (2013). IntCal13 and Marine13 Radiocarbon Age Calibration Curves 0–50,000 Years cal BP. *Radiocarbon*, *55*(4), 1869–1887. https://doi.org/10.2458/azu_js_rc.55.16947

Siccha, M., & Kucera, M. (2017). Data Descriptor : ForCenS , a curated database of planktonic foraminifera census counts in marine surface sediment samples, 1–12.

Spielhagen, R. F., Werner, K., Sørensen, S. A., Zamelczyk, K., Kandiano, E., Budeus, G., et al. (2011). Enhanced modern heat transfer to the arctic by warm atlantic water. *Science*, *331*(6016), 450–453. https://doi.org/10.1126/science.1197397

Stuiver, M., Reimer, P. J., & Reimer, R. W. (2020). CALIB 7.1. Retrieved from http://calib.org

Swift, J. H., & Aagaard, K. (1981). Seasonal transitions and water mass formation in the Iceland and Greenland seas. Deep Sea Research Part A, Oceanographic Research Papers, 28(10), 1107–1129. https://doi.org/10.1016/0198-0149(81)90050-9

Takahashi, K., & Be, A. W. H. (1984). Planktonic foraminifera: factors controlling sinking speeds. *Deep Sea Research Part A. Oceanographic Research Papers*, *31*(12), 1477–1500. https://doi.org/10.1016/0198-0149(84)90083-9